



IAFSS 12th Symposium 2017

# Experiments to provide the scientific-basis for laboratory standard test methods for firebrand exposure

Sayaka Suzuki<sup>a</sup>, Samuel L. Manzello<sup>b,\*</sup><sup>a</sup> Large Fire Laboratory Group, Research and Development Division National Research Institute of Fire and Disaster (NRIFD), Chofu, Tokyo 182-8508, Japan<sup>b</sup> Fire Research Division, Engineering Laboratory National Institute of Standards and Technology (NIST), Gaithersburg, MD 20899-8662, USA

## ARTICLE INFO

### Keywords:

Wildland-urban interface (WUI) fires  
Firebrands  
Urban fires

## ABSTRACT

Firebrand ignition of structures is a major factor in large outdoor fire spread. Standard laboratory test methods are required to evaluate and compare the performance of different building elements and/or vegetative fuels ability to resist firebrand ignition. It is important to determine full-scale assembly performance when exposed to firebrand showers since weak points in a given assembly can be investigated. Such studies will lead to determining the necessary configuration of building component mock-ups that can be used in standard laboratory test methods. The basis of this paper is to present a comparison of results from full-scale roofing assembly experiments, to mockups using the recently developed experimental capability at National Research Institute of Fire and Disaster (NRIFD). The results demonstrated that similar firebrand penetration behavior/trends were observed for mock-ups of full-scale roofing assemblies, as compared to experiments where full-scale roofing assemblies were used, all under similar wind speeds. The experimental findings presented in this paper represent an important step to develop reduced-scale test methods for firebrand exposure.

## 1. Introduction

Wildland-Urban Interface (WUI) fires have become a global issue. Japan does not have a specific problem of fires spreading from the wildlands to communities, such as the WUI fire problem [1]. After large earthquakes in Japan, many fires may be generated, leading to large scale urban fires [1]. Once a wildland fire reaches a community and ignites structures, structure-structure fire spread via firebrand generation occurs in the same manner as in post-earthquake fires [1].

Detailed investigations after these large outdoor fires have identified firebrands, or embers, as a significant source of structure ignition [1–3]. The dynamic process of multiple wind-driven firebrands landing and then being transported under non-combustible tiles/gaps as a function of time is not considered in current roofing assembly test standards [2]. Manzello et al. [4] revealed the vulnerabilities of curved ceramic tile roofing (Spanish tile roofing) assemblies to ignition under a controlled wind-driven firebrand attack using the NIST Firebrand Generator. The interested reader is referred elsewhere to a comprehensive overview of recent wind-driven firebrand research that was presented at the prior session of this symposium [4]. With many wildland fires propagated by wind-driven firebrands, the resistance of building elements to wind-driven firebrands have become a topic of great interest worldwide [5,6].

In a follow-on investigation, based on insights from the Spanish tile roofing experiments [4], concrete tile roofing assemblies (flat and profiled tile) as well as terracotta tile roofing assemblies (flat and profiled tile) commonly used in the USA, Australia, and elsewhere, were exposed to wind-driven firebrand showers [7]. The results demonstrated that firebrands penetrated between the tile gaps and melted the sarking material (see [7] for details of sarking) for both types of concrete tile roofing assemblies (flat and profiled tile) and the profiled tile terracotta roofing assembly when exposed to wind-driven firebrands. The experiments utilized a full-scale batch feed firebrand generator, capable of firebrand exposure of approximately 6 min [7]. The batch-feed firebrand generator was useful as a first step to determine if future work was required. (i.e. if firebrand penetration and melting of sarking occurred).

The objective of the present investigation was to observe the full-scale performance of tile roofing assemblies exposed to continuous firebrand showers for various wind speeds, described in detail in [8], and use those results to guide experiments using mock-ups of full-scale roofing assemblies using a recently developed reduced-scale experimental facility constructed to study firebrand ignition at the National Research Institute of Fire and Disaster (NRIFD). The overall goal was to determine if similar firebrand penetration vulnerabilities were observed for reduced-sized experiments. Such results will guide the

\* Corresponding author.

necessary configuration of roofing assembly mock-ups that can be used in standard laboratory test methods.

The recently developed experiment facility at NRIFD has not appeared in the archival literature, only a recent conference without peer-reviewed proceedings [9], since the authors feel this symposium is the most important venue for publication of this facility. It is envisioned that the development of more ignition resistant structures in large outdoor fires, not only WUI fires, but urban fires in Japan, will greatly benefit fire services as it is envisioned that firefighting resources may be better used to battle such fires, since the number of structure ignitions may be reduced significantly.

## 2. Experimental description

### 2.1. Full-scale experiments at the fire research wind tunnel facility (FRWTF)

Complete details of the full-scale roofing assembly experiments are described elsewhere [8]. However, a brief overview is provided for the reader to possess the requisite understanding necessary to follow the comparison to experiments using the reduced-scale experimental facility below.

To generate firebrand showers, the full-scale continuous feed firebrand generator was used. The description differs from descriptions available elsewhere [10] since the feeding system was redesigned to be able to generate firebrand size and mass distributions using larger wood chips in an effort to produce a wider range of exposure conditions. The device consisted of two parts: the main body and continuous feeding component. The main body of the generator was the same as prior investigations (Dragon component); the feeding system was modified to produce larger firebrands. The feeding system was connected to the main body and was equipped with two gates to prevent fire spread. A blower was connected to the main body. The blower was needed to loft and control the combustion state of the generated firebrands. The feeding parts needed to be shielded from the wind as the firebrand generator was housed inside wind tunnel during experiments.

The feeding system consisted of a pneumatic cylinder coupled to a cylindrical container where wood pieces were stored (see Fig. 1). Below the wood storage area, a plate was installed that allowed variation in the volume of wood to fall from the storage area to the first gate. When the air pressure was applied, the sliding rod of the pneumatic cylinder moved forward and separated the wood chips from the storage area to the first gate, where they were then dropped into the second gate that leads to the Dragon where they are ignited (see Fig. 1). The pneumatic cylinder was carefully selected in order to force wood pieces through and avoid jamming.

For all experiments, Japanese Cypress wood chips were used to produce firebrands (see Fig. 1). These were provided from a supplier. Wood chips were oven dried and filtered using a 10 mm mesh. These wood chips were used with the intent to produce firebrands with the mass and the projected area similar to burning structures [11]. In all experiments, the firebrands were similar to those quantified from burning structures, and these structure firebrands were used to expose the tile roofing assemblies.

As in prior experiments using the NIST Dragon, the new experimental device was installed inside the test section of the Building Research Institute's (BRI) Fire Research Wind Tunnel Facility (FRWTF). The facility was equipped with a 4 m diameter fan to produce the wind field. The cross section of the FRWTF is 5 m wide by 4 m high.

The roofing assemblies were placed 2 m from the full-scale continuous feed firebrand generator. Scoping experiments revealed that roofing assemblies at 2 m from the Dragon would receive significant firebrand showers [7,8]. The roofing assemblies were mounted on a custom stage for all experiments. The roof assemblies were constructed

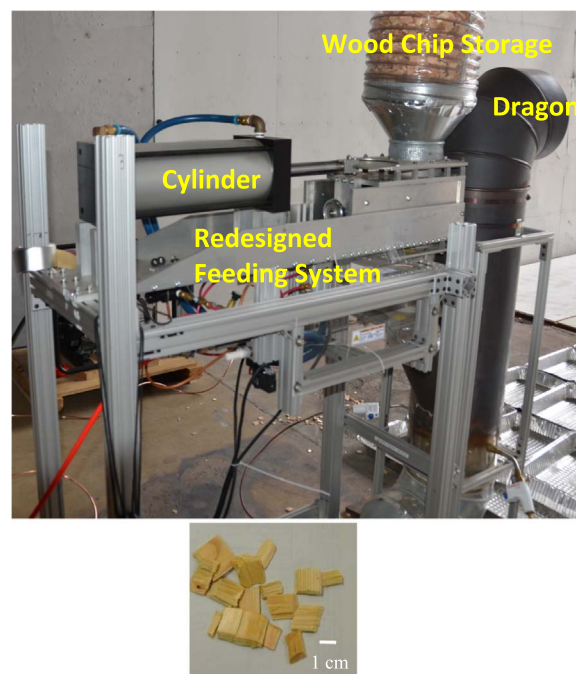


Fig. 1. Schematic of full-scale continuous feed firebrand generator. Wood chips are shown.

based on the Tile Roof Institute design manual (USA construction manual) [8]; thus counter-battens were used for all experiments.

In the case of the tile roofing assemblies, the base frame was constructed of 2×6 boards, and was lined with oriented strand board (OSB). The OSB was not oven dried; nominally 11% moisture content (MC). Felt underlayment (No. 30 felt) was applied on top of the OSB sheathing and the wood batten spacing was adjusted depending on the type of ceramic or terracotta tile roofing assembly being tested. Three types of tile roofing assemblies were used, including two concrete tile roofing assemblies (flat and profiled tiles) as well as one terracotta tile roofing assembly (flat tiles). A roof angle of 25 degrees (commonly found in practice) was used for all the roofing assemblies for direction comparison to prior work [7,8]. The overall dimensions of each roof assembly were 1.2 m by 1.2 m.

### 2.2. Reduced-scale experimental facility at NRIFD

A reduced-scale continuous feed firebrand generator was used to generate firebrand showers. To couple it with wind facility at NRIFD, the original reduced-scale continuous feed firebrand generator [12] was modified. This reduced-scale continuous feed firebrand generator consisted of two parts; the main body and continuous feeding component (see Fig. 2). The feeding part was connected to the main body and had two gates to prevent fire spread. Each gate was opened and closed alternatively. A blower was also connected to the main body for the same reason as the full-scale firebrand generator. The blower speed at the Dragon's mouth was set to 4.0 m/s. When the blower was set to provide an average velocity below 4.0 m/s measured at the exit of the firebrand generator when no wood chips were loaded, insufficient air was supplied for combustion and this resulted in a great deal of smoke being generated in addition to firebrands. Above 4.0 m/s, smoke production was mitigated but then many firebrands produced were in a state of flaming combustion as opposed to glowing combustion. In these experiments, glowing firebrands were desired to have a direct comparison to the full-scale experimental results. A longer main body was adapted so that only the firebrand generator part was above the stage, so the feeding part was not affected by wind. The efficacy of a smaller sized firebrand generator to develop continuous firebrand

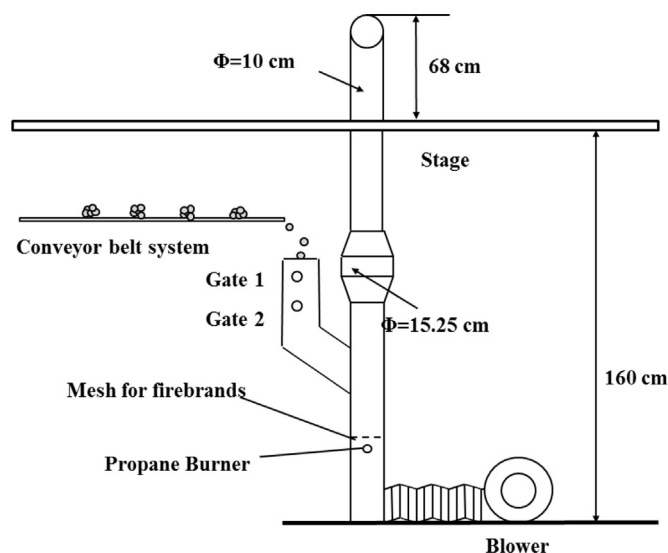


Fig. 2. Schematic of reduced-scale continuous feed firebrand generator (front view).

showers has been described in detail elsewhere [12].

A conveyor was used to feed wood pieces continuously into the device. For all tests, Japanese Cypress wood chips were used to produce firebrands. These same size wood pieces were used in the full-scale roofing assembly study and have been shown to be within projected area/mass of burning structures [8,11]. Specifics of the wood feeding rate are provided below.

As the base of the fan used to generate the wind field is located 1.6 m from the floor, the conveyor was placed under a custom stage designed for experiments when using the National Research Institute of Fire and Disaster's (NRIFD) wind facility (see Fig. 3). The flow field was measured to be within  $\pm 10\%$  over a cross-section of 2.0 m by 2.0 m. A direct comparison of the full-scale and reduced-scale continuous feed firebrand generators is shown in Fig. 4.

Experiments were conducted for two types of concrete tile roofing assemblies (flat and profiled), and one type of terracotta tile roofing assembly (flat). The dimensions of these mock-ups were half the size of the full-scale roofing assembly experiments: 0.6 m (W) and 1.2 m (L) for the concrete roofing assemblies (flat and profiled), and 0.46 m (W)

and 1.2 (L) for the terracotta tile roofing assembly (flat). This configuration was selected to investigate firebrand penetration within the center of the roofing assembly, not the leading edge. For all tile roofing assemblies, the base frame was constructed of 2×4 boards, and was lined with oriented strand board (OSB) sheathing. The OSB was not oven dried; nominally 11% MC. Felt underlayment (No. 30 felt) was applied on top of the OSB sheathing and the wood batten spacing was adjusted depending on the type of ceramic or terracotta tile roofing assembly being tested.

### 3. Results and discussion

A set of experiments was performed to obtain the fundamental characteristics of generated firebrands – mass and size. Pans filled with water were placed downstream from the NIST full-scale/reduced-scale continuous feed firebrand generator under different wind speed (6 m/s and 9 m/s). Water is necessary to suspend combustion of the firebrands. If there was no water, firebrand combustion would ensue, and the size and mass would continue to reduce. Firebrands were collected from pans by fine-mesh filters and dried in an oven at 104 °C for 16 h, until the firebrands were completely dried.

The mass and projected area of the generated firebrands at 6 m/s and 9 m/s from full-scale and reduced-scale firebrand generator is displayed in Fig. 5. The projected area of a firebrand was determined by using image analysis software. A firebrand was laid flat so that the maximum projected area of a given firebrand was measured. The photograph of the firebrand was taken along with the known scale factor. The uncertainty of the projected area was determined by the repeated measurements of well-defined objects [8] and found to be  $\pm 10\%$ . The mass of each firebrand was measured by a scale with 0.001 g resolution. The uncertainty of the mass was determined by the repeated measurements of the known mass and found to be  $\pm 1\%$ . The characteristics of firebrands in this study for all experiments were observed to be similar regardless of the firebrand generator (full-scale or reduced-scale), and wind speeds (6 m/s or 9 m/s). The average mass and standard deviation of each firebrand for all was obtained to be  $0.03 \text{ g} \pm 0.02 \text{ g}$ .

#### 3.1. Full-scale roofing assemblies

Experiments with different feeding rate were performed for the optimal conditions to produce continuous firebrand attack. 150 g to 200 g of wood pieces loading every 15 s were found to produce copious amounts of firebrands continuously to ignite building materials. In this experimental series, 170 g of Japanese cypress chips were loaded into the full-scale NIST Dragon every 15 s (680 g/min). The number flux at a feeding rate of 170 g every 15 s was measured by counting firebrands produced from the exit of the device. The number of firebrands produced were counted every frame and summed up every second. It took 20 s to start generating firebrand showers and 150 s to reach the stable firebrand production of  $533/\text{m}^2 \text{ s}$  at this feeding rate [8]. Therefore, the mass flux of generated firebrands was calculated to be  $16 \text{ g}/\text{m}^2 \text{ s}$  by multiplying the number flux and the average mass of each firebrand at a feeding rate of 680 g/min [8].

The number flux of firebrands landing on the tile roofing assembly was also measured in the same manner [7]. The average number flux of firebrands landing on the roof assembly was measured at  $10/\text{m}^2 \text{ s}$ , therefore the mass flux of firebrands landing on the roof assembly were calculated to be  $0.3 \text{ g}/\text{m}^2 \text{ s}$ . Only 35% of firebrands produced from the Dragon arrived at the surface of the roofing assembly. In previous experiments with original batch feed firebrand generator [7], the arriving mass flux of firebrands to the roofing assemblies was the same.

It was observed that firebrands accumulated in the gaps of the tiles for all types of roof tile assemblies in this study. Firebrands that accumulated burned until they were small enough to penetrate under the roofing tiles, and finally reached onto the underlayment/counter-

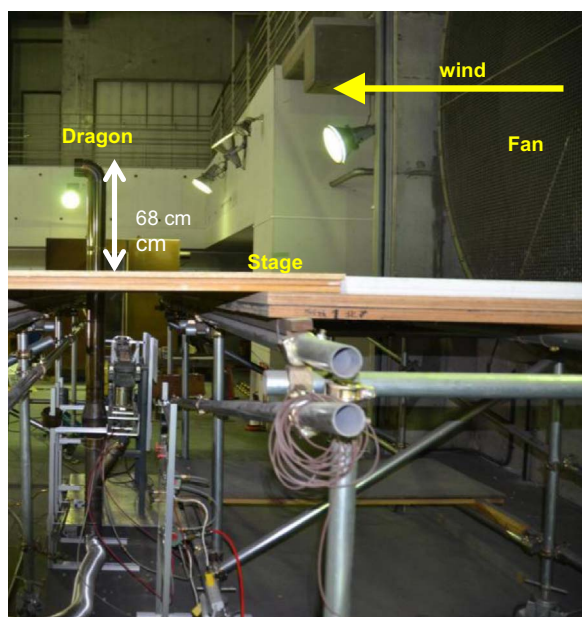


Fig. 3. Picture of NRIFD experimental facility (side view). The stage dimensions were 5.5 m wide, 6.4 m long, with a height of 1.6 m.

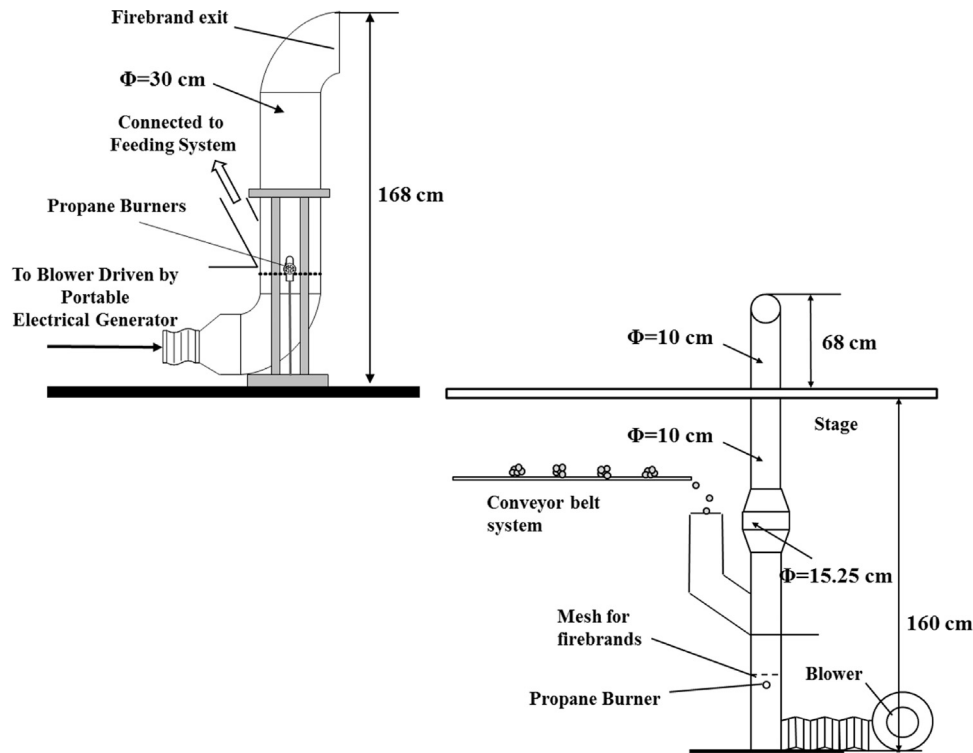


Fig. 4. Direct comparison of size of two Dragons. (Left: Full-scale continuous feed firebrand generator Right: reduced-scale continuous feed firebrand generator).

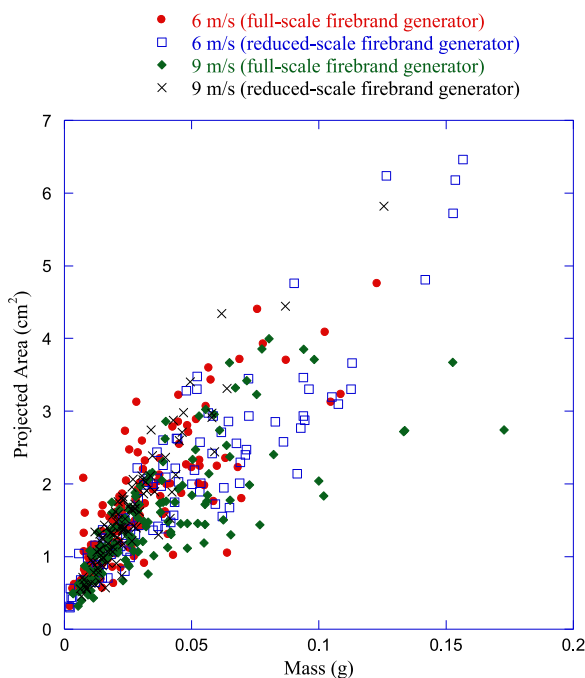


Fig. 5. Size and mass distribution of generated firebrands for full-scale and reduced-scale firebrand generators (comparison at 6 m/s and 9 m/s). The sizes of Japanese Cypress wood chips used for firebrand generation (before combustion) were  $28 \pm 8$  mm (length),  $18 \pm 6$  mm (width), and  $3 \pm 1.0$  mm (thickness) (average  $\pm$  standard deviation), respectively.

batten system. The most severe penetration was observed to occur on the surface of the roofing assembly, not at the leading edge.

To identify the severity of penetration for each condition, the number of firebrands deposited on the underlayment/counter-batten, after penetrating under the roof tiles, was counted for all experiments (Fig. 6). The uncertainty was determined to be 5% by repeated

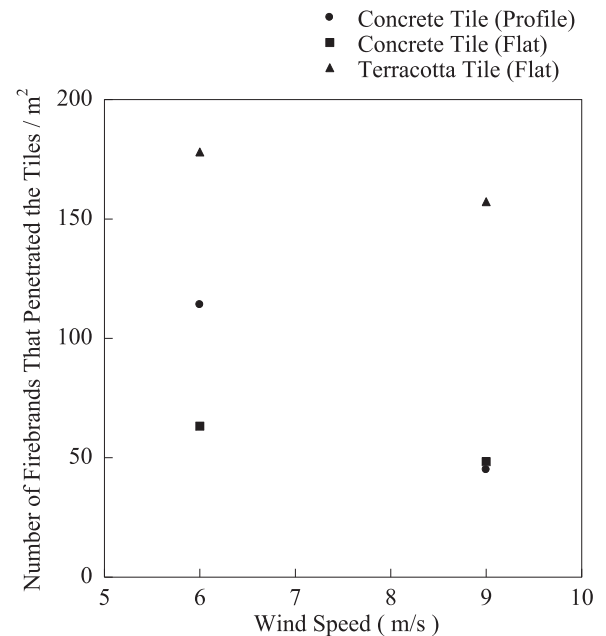


Fig. 6. The number of firebrands that penetrated per area the full-scale tile roofing assemblies as a function of applied wind speed (20 min firebrand exposure; recalculated data from Suzuki et al. [8]).

experiments. The flat terracotta tiles were found to have the most firebrand penetration, as compared to the other types of concrete tiles (profiled and flat). The amount of firebrand penetration for the profiled concrete tiles was drastically reduced from 6 m/s to 9 m/s wind speed compared to those for the flat concrete tiles. Under 6 m/s wind speed, many firebrands were accumulated at the tile gaps due to the raised profile, and eventually penetrated. However, as the wind speed increased, less firebrands were capable to accumulate at the tile gaps, which resulted in less penetration at the higher wind speed. It was also observed that firebrands deposited on the underlayment/counter-





Concrete Tile (profiled)  
0.6 m by 1.2 m



Concrete Tile (flat)  
0.6 m by 1.2 m



Terracotta Tile (flat)  
0.46 m by 1.2 m

**Fig. 7.** Three different types of tile roofing assembly mock-ups experimented used. In each case, these are half the size of the full-scale roofing assemblies described above.

batten caused smoldering ignition on the counter-battens, but did not transition to flaming ignition.

### 3.2. Mock-ups of full-scale roofing assemblies

As indicated, a conveyor was used to feed wood pieces continuously into the device. The conveyor belt was operated at 1.0 cm/s, and wood pieces were put on the conveyor belt at 12.5 cm intervals. The wood feed rate was fixed at 80 g/min, near the upper limit of reduced-scale firebrand generator. These same size wood pieces were used in the full-scale roofing assembly study. Fig. 5 displays the projected area and mass of the generated firebrands at 6 m/s and 9 m/s using the same analysis methods described above.

Fig. 7 shows three different types of tile roofing assembly mock-ups experimented with, and Figs. 8–10 are typical photos of experiments. Similar to the full-scale experiments, the duration of the firebrand flux was fixed at 20 min and the wind speed was varied from 6 m/s to 9 m/

s. For both types of concrete tiles (flat and profiled), as well as the terracotta (flat) roofing assembly, firebrands were observed to accumulate in the gaps of the tiles. The firebrands continued to burn until they were able to penetrate the tile gaps and pass onto the underlayment/counter-batten system. In all tiles that were experimented upon, the most severe penetration occurred on the surface of the roofing assembly, not at the leading edge.

To attempt to quantify the degree of penetration, the number of firebrands that penetrated the tiles, and deposited onto the underlayment/counter-batten system was counted as function of wind speed for each tile roofing assembly. These results are shown in Fig. 11. As can be seen, the terracotta tiles (flat), resulted in the most firebrand penetration. Firebrand penetration resulted in smoldering ignition of the counter-batten system but a transition to flaming ignition was not observed in any experiments (see Fig. 12).

It is important to note that similar firebrand penetration trends were observed between the full-scale roofing assembly experiments and the roofing section mock-ups. The terracotta tiles (flat) resulted in the most penetration at 6 m/s, and the concrete tiles (flat) resulted in the least firebrand penetration at 6 m/s. Fig. 13 displays a simplified schematic of the physics of the firebrand penetration process. As discussed above, firebrands accumulated on the roof tile gaps first. As combustion continued, firebrands become smaller, eventually penetrating between the gaps of the roof tiles, and reached the underlayment/counter-batten system. Once reaching there, firebrands accumulated either on the underlayment or around the counter batten system, which resulted in smoldering ignitions on the counter-batten system in the latter case (shown in Fig. 12).

The total number of firebrands that penetrated the roofing section mock-ups was considerably less than the full-scale experiments. This was expected since the feeding rate of wood chips was 80 g/min, or 8.5 times less than the full-scale experiments. To further understand these differences, the arrival number flux of firebrands was compared between the full-scale experiments to the mock-up roofing assemblies. In the case of the full-scale roofing experiments, the average arrival number flux was 10/m<sup>2</sup> s as compared to 7/m<sup>2</sup> s for the mock-ups. It is natural that overall less firebrand penetration (total number) was observed for the mock-up roofing assemblies since: less firebrands actually arrive, and once they arrive, there are less tile gaps for the firebrands to penetrate.



**Fig. 8.** Concrete tile (profiled) roofing assembly exposed to firebrand showers at 6 m/s. The height of the firebrand generator was 68 cm from the base of the stage. The distance from the firebrand generator to the leading edge of roofing assembly was 0.5 m. Significant firebrand arrival occurred at this generator–roof distance.



**Fig. 9.** Concrete tile (flat) roofing assembly exposed to firebrand showers at 6 m/s. The height of the firebrand generator was 68 cm from the base of the stage. The distance from the firebrand generator to the leading edge of roofing assembly was 0.5 m.



**Fig. 10.** Terracotta tile (flat) roofing assembly exposed to firebrand showers at 6 m/s. The height of the firebrand generator was 68 cm from the base of the stage. The distance from the firebrand generator to the leading edge of roofing assembly was 0.5 m.

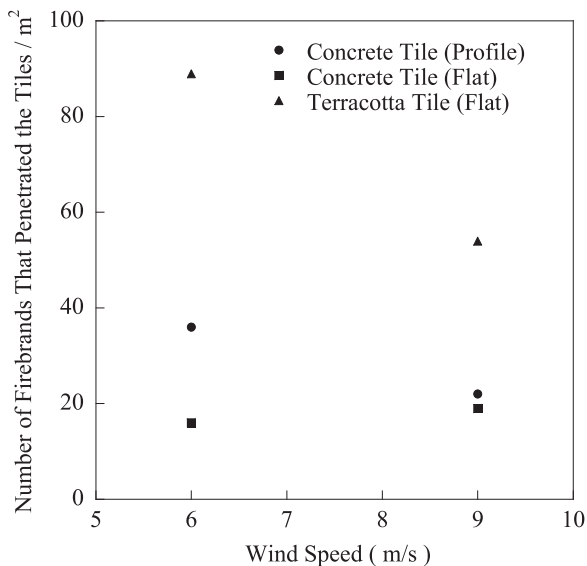


**Fig. 11.** The number of firebrands that penetrated the tile roofing assemblies per area as a function of applied wind speed (20 min firebrand exposure). Firebrands were counted after the tiles were removed.

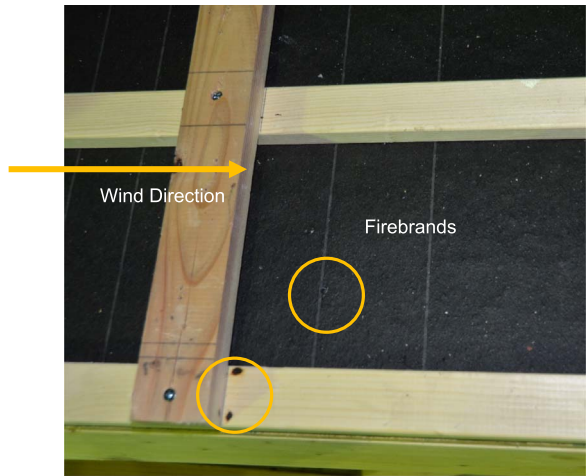


**Fig. 12.** The Terracotta tile (flat) roofing assembly exposed to firebrand showers at 6 m/s. 20 min firebrand exposure. Smoldering ignition of battens - no transition to flaming ignition observed. The batten ignition is circled as are the firebrands that penetrated the tiles.

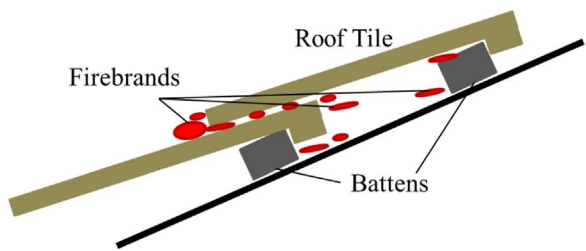


**Fig. 13.** Simple schematic as to the mechanism of firebrand penetration under roof tiles. Please not there is no attempt to highlight actual tile overlap dimensions, or roofing pitch, but rather demonstrate the physics of the penetration process.

4. Summary

These experiments have demonstrated that similar firebrand penetration behavior/trends were observed for mock-ups of full-scale roofing assemblies, as compared to experiments where full-scale roofing assemblies were used, all under similar wind speeds. At the same time, the penetration data will serve as part of database of roofing assembly performance to continuous firebrand exposure.

For the roofing assembly studies, the total exposure time of firebrand showers was selected to be 20 min, about three times longer than was possible using prior bath-fed firebrand generators. Naturally, a representative time for firebrand exposure depends on

many factors in actual large outdoor fires, such as WUI and urban fires. It is believed that different durations of firebrand exposure could serve as the basis for a rating system for use in standard test methods for roofing assembly performance. In particular, quantifying firebrand exposure from actual WUI and urban fires is required to determine representative firebrand exposure duration, and these will be helpful to *provide bounds of exposure severity* to wind-driven firebrand showers. This premise is analogous to what is currently done for various fire safety test methods (*i.e.* Class A assembly indicates most ignition resistant). Efforts are currently underway to develop a field deployable measurement device to quantify real scale firebrand number fluxes.

While the present experimental campaign has focused on roofing assembly exposure to firebrand showers, post-fire studies also suggest that attached building components may provide additional pathways for structures to ignite in WUI fires [3,13]. Examples of attached building components include decking and fencing assemblies. Recent full-scale experimental investigations by the authors demonstrated that both wood fencing assemblies and wood decking assemblies may be ignited by firebrand showers [10,14]. Work is currently underway to compare ignition vulnerabilities observed from full-scale experiments to mock-ups of full-scale fencing and decking assemblies using the NRIFD facility, in a similar manner to what has been completed here for roofing assemblies.

The experimental findings presented here represent an important step to develop reduced-scale test methods for firebrand exposure. Obtaining insights into ignition behavior from reduced sized experiments is a desirable tool, as understanding firebrand attack on buildings remains a complex and difficult task. The development of these unique experimental facilities is beginning to unravel the complex problem of firebrand exposure to building components.

## Acknowledgements

Mr. Marco Fernandez of NIST's Engineering Laboratory (EL) is acknowledged for shipping materials for the experiments. The support of Dr. Daisaku Nii (Kyoto University, formerly of the Building Research Institute, Japan) was helpful to complete the full-scale experimental

campaign focused on roofing assemblies in this work. Dr. Ichiro Hagiwara, Group Leader, Department of Fire Safety Engineering, at the Building Research Institute (Japan) is appreciated for helpful discussions.

## References

- [1] S.L. Manzello, et al., Workshop for fire structure interaction and urban and wildland-urban interface(WUI) fires – operation tomodachi fire research, *Fire Saf. J.* 59 (2013) 122–131. <http://dx.doi.org/10.1016/j.firesaf.2013.03.021>.
- [2] S.L. Manzello, E.I.D. Foote, Characterizing firebrand exposure from wildland-urban interface (WUI) fires: results from the 2007 Angora fire, *Fire Technology* 50 (2014) 105–124. <http://dx.doi.org/10.1007/s10694-012-0295-4>.
- [3] A. Maranghides, et al., A case study of a community affected by the waldo fire – event timeline and defensive actions, *NIST TN1910* (2015). <http://dx.doi.org/10.6028/NIST.TN.1910>.
- [4] S.L. Manzello, Enabling the investigation of structure vulnerabilities to wind-driven firebrand showers in wildland urban interface (WUI) fires, *Fire Saf. Sci.* 11 (2014) 83–96. <http://dx.doi.org/10.3801/IAFSS.FSS.11-83>.
- [5] S.L. Manzello, (Invited Guest Editor), (2014) Special Issue on Wildland-Urban Interface (WUI) Fires, *Fire Technology*, 50, pp. 7–8. <http://dx.doi.org/10.1007/s10694-012-0319-0>.
- [6] S.L. Manzello, S.L. Quarles, (Guest Editors) (2017) Special Section on Structure Ignition in Wildland-Urban Interface (WUI) Fires, *Fire Technology*, 52, pp. 425–427. <http://dx.doi.org/10.1007/s10694-016-0639-6>.
- [7] S.L. Manzello, The performance of concrete tile and terracotta tile roofing assemblies exposed to wind-driven firebrand showers, *NIST Tech. Note* 1794 (2013). <http://dx.doi.org/10.6028/NIST.TN.1794>.
- [8] S. Suzuki, S.L. Manzello, D. Nii, The performance of wood and tile roofing assemblies exposed to continuous firebrand assault, *Fire Mater.* 41 (2017) 84–96. <http://dx.doi.org/10.1002/fam.2372>.
- [9] S.L. Manzello, S. Suzuki, Firebrand Ignition in Large Outdoor Fires: The Use of Full-Scale Experiments to Guide the Development of Laboratory Standard Test Methods, in: *Proceedings of the 14th International Conference on Fire Science and Engineering (Interflam)*, Interscience Communications, 2016.
- [10] S. Suzuki, et al., Ignition of wood fencing assemblies exposed to continuous-wind driven firebrand showers, *Fire Technol.* 52 (2016) 1051–1067. <http://dx.doi.org/10.1007/s10694-015-0520-z>.
- [11] S.L. Manzello, S. Suzuki, Generating wind-driven firebrand showers characteristic of burning structures, *Proc. Combust. Inst.* 36 (2017) 3247–3252. <http://dx.doi.org/10.1016/j.proci.2016.07.009>.
- [12] S. Suzuki, S.L. Manzello, On the development and characterization of a reduced-scale continuous feed firebrand generator, *Fire Saf. Sci.* 10 (2011) 1437–1448. <http://dx.doi.org/10.3801/IAFSS.FSS.10-1437>.
- [13] S.L. Quarles, et al., Lessons learned from Waldo Canyon: fire adapted communities mitigation assessment Team findings, *Insur. Inst. Bus. Home Saf.* (2013).
- [14] S.L. Manzello, S. Suzuki, Exposing decking assemblies to continuous wind-driven firebrand showers, *Fire Saf. Sci.* 11 (2014) 1339–1352. <http://dx.doi.org/10.3801/IAFSS.FSS.11-1339>.